Bioactive Materials 53 (2025) 32–44

Contents lists available at ScienceDirect

Bioactive Materials

journal homepage: www.keaipublishing.com/en/journals/bioactive-materials

Oral microbiota-regulating and inflammation-targeted polymersome-hydrogels for RNAi therapy of ulcerative colitis

Huan He [a], Xinyi Dong [b], Li Cao [a], Yongjie Sha [b], Yinping Sun [b], Songsong Zhao [b], Fenghua Meng [b], Zhiyuan Zhong [a,b,*]

[a] College of Pharmaceutical Sciences and State Key Laboratory of Radiation Medicine and Protection, Soochow University, Suzhou, China
[b] Biomedical Polymers Laboratory, College of Chemistry, Chemical Engineering and Materials Science, Soochow University, Suzhou, China

ARTICLE INFO

Keywords:
Intestinal flora
siRNA delivery
Targeted nanoparticles
Eatable hydrogels
Autoimmune diseases

ABSTRACT

The treatment of ulcerative colitis is harassed by its intricate pathogenesis and the harsh gastrointestinal environment. Herein, oral microbiota-regulating and inflammation-targeted polymersome-hydrogels are developed by incorporating gallic acid and tumor necrosis factor α-specific siRNA-encapsulated polymersomes (GA-siTNFα-PS) into self-healable and eatable hydrogels (SHE-Gel) formed from thiolated sodium alginate and dopamine-modified oxidized inulin (DA-OIn) for oral RNAi therapy of ulcerative colitis. SHE-Gel is stable in stomach, resides in the intestine, and degrades in the colon by colon-specific inulinase. DA-OIn endows SHE-Gel anti-oxidative stress and prebiotic activities that modulate the diversity of gut microbiota. GA-siTNFα-PS released in the colon can adhere to the inflamed sites, resulting in selective delivery of siTNFα to macrophages. GA eliminates ROS and further protects siTNFα from degradation. Remarkably, GA-siTNFα-PS/SHE-Gel not only effectively blocks the progression of inflammation but also maintains the homeostasis of gut microbiota in the ulcerative colitis model. GA-siTNFα-PS/SHE-Gel can further combine with anti-TNFα antibody, restoring the intestinal immune and gut microbiota homeostasis in an advanced model of colitis in mice. The polymersome-hydrogels with effective suppression of intestinal inflammation and modulation of gut microbiota provide a versatile and powerful strategy for treatment of ulcerative colitis.

1. Introduction

Ulcerative colitis (UC) is an autoimmune disease with relapsing, refractory, and uncontrolled inflammatory responses in the ileum, rectum, and colon [1–3]. Over the past decade, biological therapy with antibodies targeting to the excessive inflammatory cytokines (such as anti-tumor necrosis factor α (TNFα) or interleukin-12/23) has been intensively investigated as a therapeutic option for UC patients, especially in cases where the disease is refractory or intolerant to conventional agents [4–6]. Biological targeted therapy has yielded promising therapeutic outcomes in the preclinical and clinical treatment of UC, but it may carry risks of immunogenicity, poor circulation stability, high cost, and antibody resistance upon repetitive administration [7–10]. RNA interference (RNAi) nanodrugs can inhibit protein production from the source by degrading the mRNA of the target gene, and may inhibit the function of the target protein more effectively than monoclonal antibody drugs [11,12]. However, efficient delivery of RNAi nanodrugs to the colon remains a great challenge due to their liability to degradation in the complex physiological environment in the body [13,14]. In addition, since UC is a multifactorial and multistep process, blocking only a single inflammatory cytokine while ignoring important inducing factors, including oxidative stress and bacterial flora disturbance [15,16], may not suffice to maintain clinical remission and achieve long-term efficacy.

Oral administration is convenient, safe, and able to deliver drugs to the intestinal mucosa, making it a viable alternative to systemic administration for the treatment of UC [17,18]. Eatable polysaccharide hydrogels, based on e.g. alginate, chitosan, and hyaluronic acid, are promising oral drug delivery vehicles because they protect drug from degradation by gastric acid and enzymes to certain extent [19–21]. For example, pH-responsive sodium alginate hydrogels are one of the most popular intestinal delivery vehicles, because they gelate under

Peer review under the responsibility of editorial board of Bioactive Materials.
* Corresponding author. College of Pharmaceutical Sciences and State Key Laboratory of Radiation Medicine and Protection, Soochow University, Suzhou, China.
E-mail address: zyzhong@suda.edu.cn (Z. Zhong).

https://doi.org/10.1016/j.bioactmat.2025.06.039
Received 6 April 2025; Received in revised form 5 June 2025; Accepted 20 June 2025
Available online 4 July 2025

extremely acidic conditions in the stomach and degrade at neutral to basic pH conditions in the small intestine and colon [22,23]. Inulin can maintain structural stability in the gastrointestinal tract and be degraded by colon-specific inulinase, and inulin metabolites have prebiotic activity and can regulate intestinal flora [24,25]. Thus, inulin-based hydrogels have been constructed for colon drug delivery and flora regulation [26]. These oral hydrogels, though interesting for UC treatment, have met several challenges: (1) poor tissue adhesion and quick clearance from the body due to diarrhea in UC patients; (2) weak compressive strength leading to premature drug release under gastrointestinal compression (up to 13 kPa [27,28]); (3) inadequate self-healing ability, leading to gel fragmentation; and (4) low capability of removing ROS and regulating microbiota functions.

Here, we propose oral microbiota-regulating and inflammation-targeted polymersome-hydrogels for RNAi therapy of ulcerative colitis (Fig. 1). Gallic acid and TNFα-specific siRNA were encapsulated within polymersomes (GA-siTNFα-PS) and then loaded into self-healable and eatable hydrogels (SHE-Gel) formed from thiolated sodium alginate (SH-SA) and dopamine-modified oxidized inulin (DA-OIn). The polymersome-hydrogel system GA-siTNFα-PS/SHE-Gel was designed with the following properties: (i) nano-enhanced mechanical property, self-healing property and mussel-inspired adhesive property, which enable resistance to gastrointestinal extrusion and strong adherence in the colon, thus avoiding rapid excretion due to diarrhea in UC models; (ii) pH and colonic enzyme responsiveness, which enables resistance to the extremely acidic stomach environment and colon-specific degradation and drug release triggered by inulinase in the colon; (iii) DA-antioxidative stress and prebiotic activities endowed by OIn, modulating the gut microbiota; and (iv) targeted delivery property of GA-siTNFα-PS to the inflamed colon and intracellular release of GA and siTNFα within macrophages, resulting in effective ROS-scavenging and TNFα silencing, and ultimately inhibiting the overactive intestinal immune response. GA, as a natural polyphenol, has been reported to possess ROS scavenging ability and is widely used as an antioxidant and anti-inflammatory agent [29].

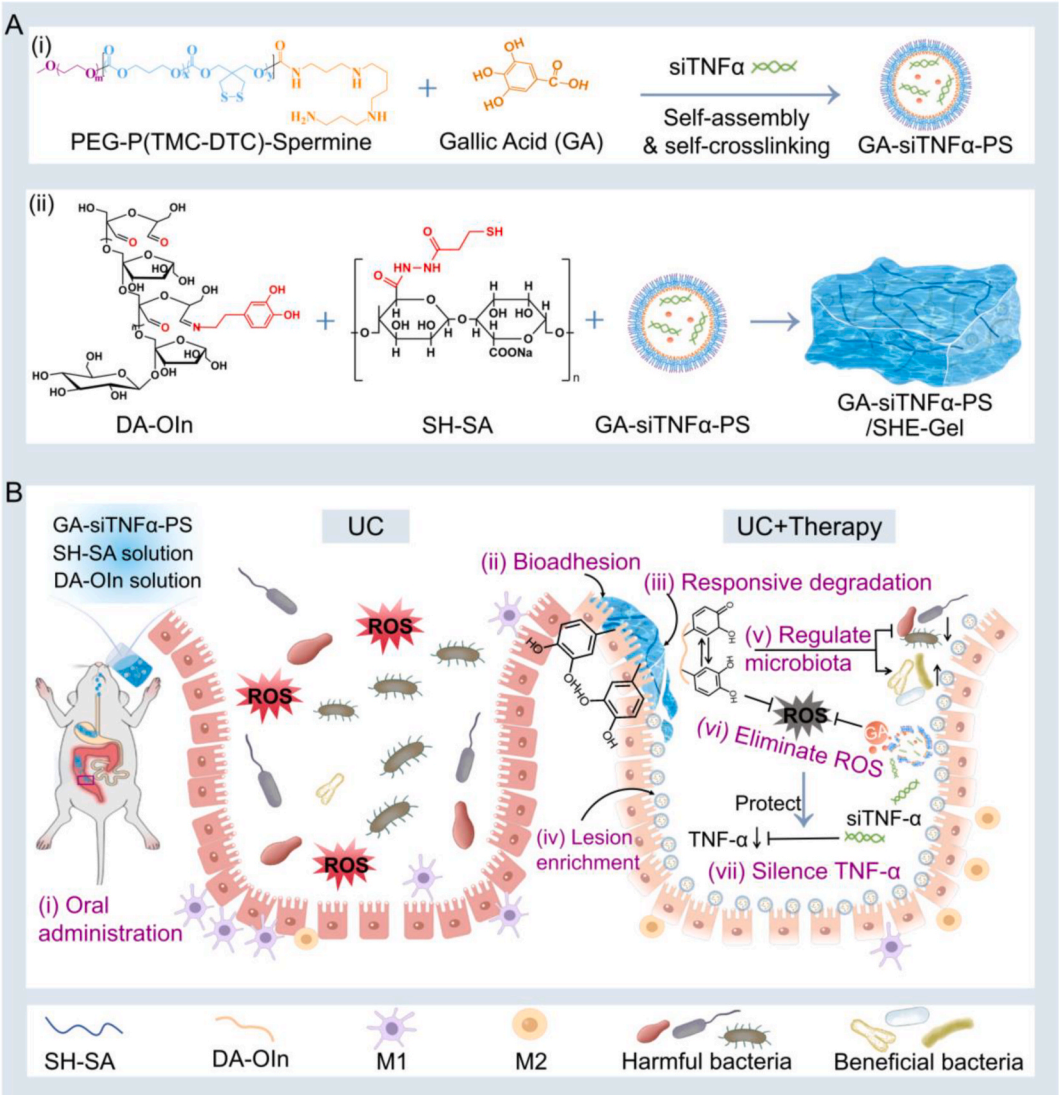

Fig. 1. Schematic illustration of the synthesis of GA-siTNFα-PS/SHE-Gel and its application in UC treatment. A) Synthesis of (i) GA-siTNFα-PS and (ii) GA-siTNFα-PS/SHE-Gel. B) C) Utilization of GA-siTNFα-PS/SHE-Gel for UC therapy. (i) GA-siTNFα-PS/SHE-Gel forms in situ in the stomach after intragastric administration of a mixture of SH-SA solution and DA-OIn solution containing GA-siTNFα-PS. It can smoothly pass through the gastrointestinal tract, (ii) adhere to the intestine, and (iii) responsively degrade in the inflammed colon, (iv) where GA-siTNFα-PS is released and selectively delivered siTNFα and GA to macrophages. (v-vii) The mechanism of GA-siTNFα-PS/SHE-Gel treatment of UC is as follows. (v) DA-OIn regulates intestinal flora and (vi) inhibits intestinal oxidative stress. (vi-vii) GA-siTNFα-PS are internalized by macrophages, and the released GA clears intracellular ROS to protect the integrity of siTNFα, effectively silencing TNFα.

2. Results and discussion

2.1. Construction and characterization of GA-siTNFα-PS/SHE-gel

GA-siTNFα-PS was fabricated by self-assembly of GA and siTNFα within poly (ethylene glycol)-b-poly (trimethylene carbonate-co-dithiolane trimethylene carbonate)-spermine (PTD-sp) nanovesicles. The synthesis, structural characterization, and physicochemical properties of PTD-sp were reported in our earlier work [30]. The siRNA encapsulation efficiency, zeta potential, and particle size of GA-siTNFα-PS were evaluated. The results demonstrated that siRNA encapsulation efficiency slightly increased as the mass ratio of GA to PTD-sp increased. When the GA-to-PTD-sp mass ratio reached 1:40, the siRNA encapsulation efficiency rose to 91.0 %, while the GA loading content was 45.9 %. (Fig. 2A; Fig. S1, Supporting Information). The zeta potential of GA-siTNFα-PS was more negative than that of the siTNFα-PS (−0.8 mV) without GA, indicating that GA was successfuly loaded into the nanovesicles (Fig. 2B). The particle size of GA-siTNFα-PS was approximately 50 nm (Fig. 2C), similar as siTNFα-PS. GA also has no effect on morphology and GA-siTNFα-PS exhibited a vesicle-like morphology, consistent with the structure of siTNFα-PS (Fig. 2D; Fig. S2, Supporting Information).

The GA-siTNFα-PS/SHE-Gel formed in situ through dynamic reversible crosslinking between the aldehyde groups of DA-OIn and the thiol groups of SH-SA (Fig. 2E; Figs. S3 and S4, Supporting Information). The gelation time could be adjusted by varying the DA-OIn concentration (Fig. 2F and G). The gelation time decreased with increasing DA-OIn content, reaching 30 s at 6 wt% DA-OIn concentration. The encapsulation efficiency of GA-siTNFα-PS within SHE-Gel was nearly 100 % (Fig. 2H). SEM images showed that the GA-siTNFα-PS/SHE-Gel had a porous network structure, with pore size decreasing as DA-OIn concentration increased (Fig. S5, Supporting Information).

DA-OIn, SH-SA, and GA-siTNFα-PS were mixed and could be continuously injected into a culture dish using a 1 mL syringe with a 0.5 mm diameter needle. A filamentous strip was readily extruded from the needle, forming the letters "YBH" in the culture dish (Fig. 2I). Moreover, DA-OIn, SH-SA, and GA-siTNFα-PS formed gel in situ within the mouse stomach (Fig. 2J). Additionally, GA-siTNFα-PS/SHE-Gel also exhibited self-healing properties (Fig. 2K), showing the quick fusion of two halves of GA-siTNFα-PS/SHE-Gel at 37 °C within 2 min.

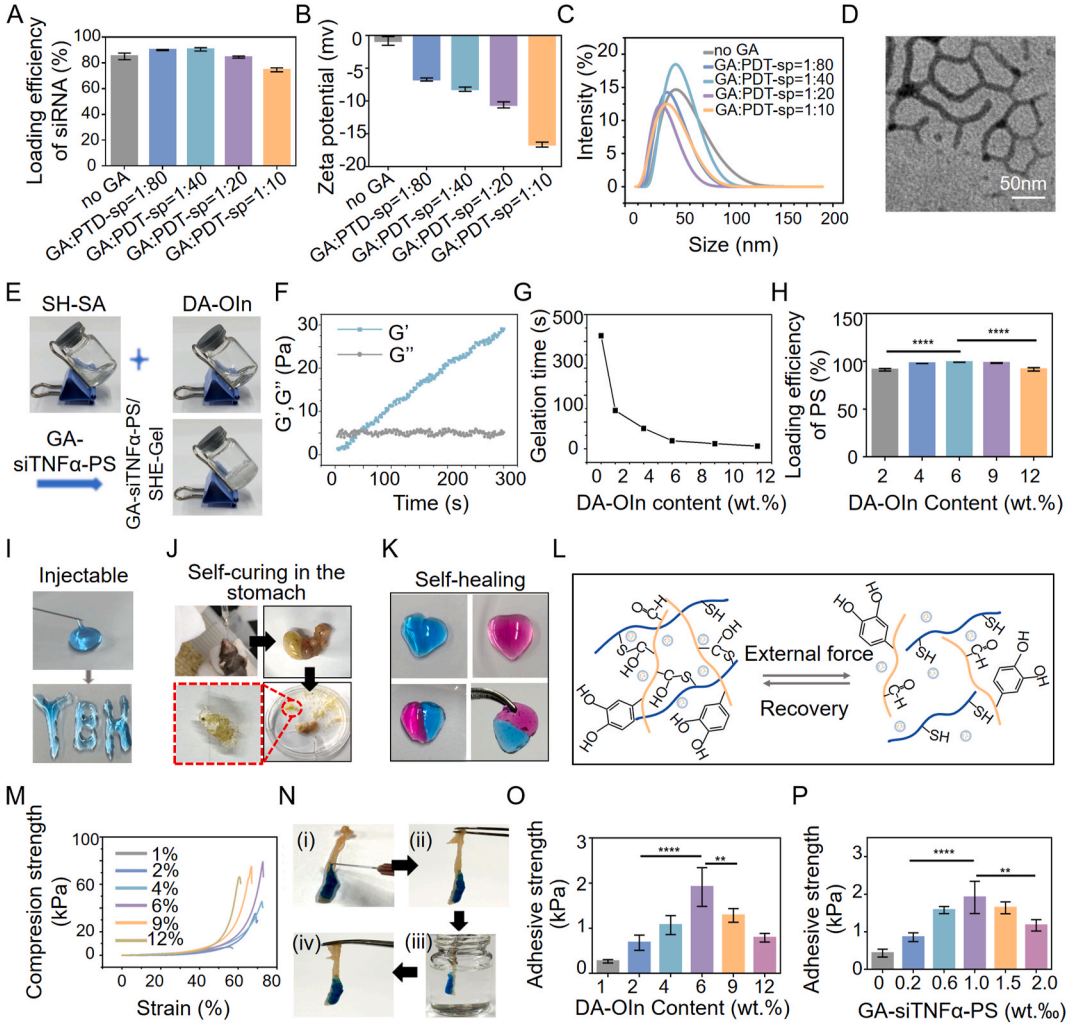

Fig. 2. Characterization of GA-siTNFα-PS/SHE-Gel. A) The siRNA loading efficiency, B) zeta potential, C) size of GA-siTNFα-PS with different mass ratio of GA and PDT-sp (n = 3). D) The TEM image of GA-siTNFα-PS. E) Photographs depicting the self-curing process of GA-siTNFα-PS/SHE-Gel. F) Rheological properties of GA-siTNFα-PS/SHE-Gel. G) Gelation time of GA-siTNFα-PS/SHE-Gel with different concentration of DA-OIn. H) Encapsulation efficiency of GA-siTNFα-PS in SHE-Gel (n = 3). I) Injectable property of GA-siTNFα-PS/SHE-Gel. J) Self-curing process of GA-siTNFα-PS/SHE-Gel in the mouse stomach. K) Self-healing ability illustration and L) mechanism of GA-siTNFα-PS/SHE-Gel. M) Compressive strength of the GA-siTNFα-PS/SHE-Gel with varying concentrations of DA-OIn. N) Robust adhesion of GA-siTNFα-PS/SHE-Gel (dyed with blue ink) to mouse colon. Adhesion strength of GA-siTNFα-PS/SHE-Gel with different concentration of O) DA-OIn and P) GA-siTNFα-PS on pigskin (n = 3) (Data are presented as the mean ± SD; ** and **** indicate significance at $p < 0.01$ and $p < 0.0001$, respectively).

2.2. Mechanical properties of GA-siTNFα-PS/SHE-Gel

The self-healing properties of GA-siTNFα-PS/SHE-Gel were quantitatively analyzed using rheological measurements (Fig. S6A, Supporting Information). GA-siTNFα-PS/SHE-Gel was in a gelation state (G'>G″) at a low strain of 10 %. However, when subjected to a strain of 550 % (exceeding the critical strain value), the hydrogel network was swiftly disrupted (G'<G″). Upon cessation of the high shear rate, the G′ and G″ of the hydrogel recovered to 100 % within seconds (Fig. S6B, Supporting Information). The robust self-healing ability of GA-siTNFα-PS/SHE-Gel stems from the dynamic and reversible bonds between thiol groups in SH-SA and aldehyde groups in DA-OIn (Fig. 2L). The self-healing performance of GA-siTNFα-PS/SHE-Gel is beneficial for re-assembling ruptured hydrogel fragments in the colon instead of rapid excretion from the body.

The mechanical properties of the hydrogel are crucial for

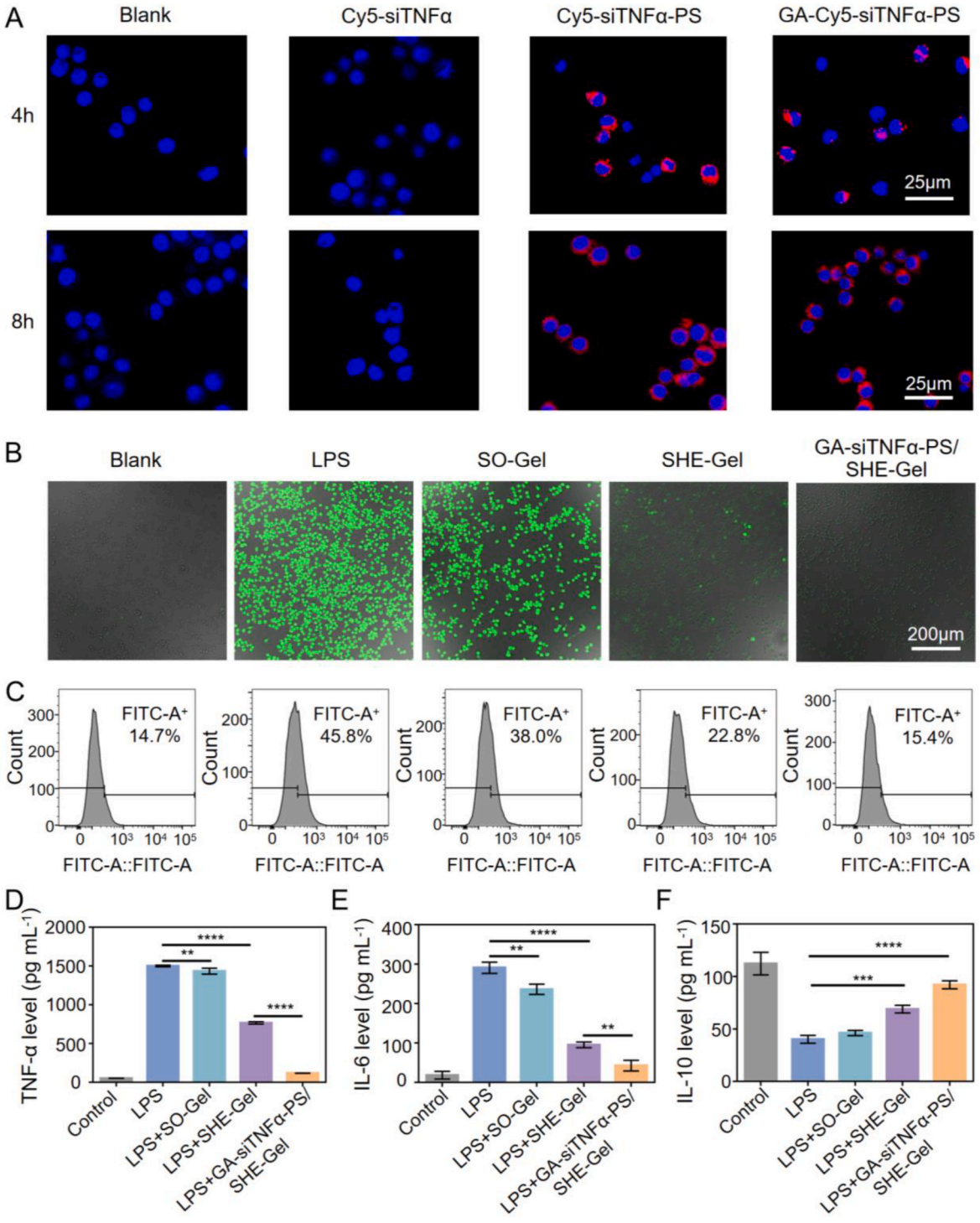

Fig. 3. Antioxidant and anti-inflammatory ability of GA-siTNFα-PS/SHE-Gel. A) CLSM images of LPS-stimulated RAW264.7 cells after incubation with Cy5-siTNFα, Cy5-siTNFα-PS, GA-Cy5-siTNFα-PS for 4 h or 8 h. Scale bar, 25 μm. B) Intracellular ROS staining images and C) flow cytometry analysis of DCFH-labeled RAW264.7 cells post different treatments. Scale bar, 200 μm. D-F) ELISA results of extracellular expression of TNF-α, IL-6, and IL-10 (n = 3). (Data are presented as the mean ± SD; **, ***, and **** indicate significance at $p < 0.01$, $p < 0.001$, and $p < 0.0001$, respectively).

maintaining structural integrity during intestinal extrusion [27]. Compression test results showed that GA-siTNFα-PS/SHE-Gel exhibited enhanced compressive strength with increating the DA-OIn content from 1 to 6 wt% (Fig. 2M; Fig. S7A, Supporting Information), by augmenting crosslinking density. However, compressive strength decreased with DA-OIn concentrations exceeding 6 wt%, probably due to the cracks formed in hydrogels with high cross-linking density and accelerated rupture under compression (Fig. S8, Supporting Information). In addition, the content of GA-siTNFα-PS also affects to certain degree the compressive strength, which increased with GA-siTNFα-PS contents from 0 to 1.0 wt‰ (Fig. S7B, Supporting Information), but not at contents exceeding 1.0 wt‰. This nano-enhanced mechanical properties was reported earlier [31], while at very high concentration of GA-siTNFα-PS hydrogel might develop cracks. Additionally, GA-siTNFα-PS/SHE-Gel also exhibited excellent anti-swelling properties with the contents of DA-OIn and GA-siTNFα-PS of 6 wt% and 1.0 wt‰, respectively (Fig. S9, Supporting Information).

GA-siTNFα-PS/SHE-Gel displayed bioadhesion properties to various tissues, due to the large number of catechol groups within the hydrogel network [32,33]. The results showed that the hydrogel did not fall off the colon tissue at perpendicular position, even soaked in PBS (Fig. 2N). The hydrogel also showed good adhesion to various biological tissues and substrates (Fig. 2O and P; Figs. S10 and 11, Supporting Information). Furthermore, the adhesion strength increased with DA-OIn contents from 1 to 6 wt%, as a higher DA-OIn content provided more catechol groups in the hydrogel, while not at DA-OIn content exceeding 6 wt%, owing to the reduced accessibility of dopamine groups at highly cross-linked hydrogel. Additionally, the strongest adhesion of the hydrogel was also obtained at GA-siTNFα-PS content of 1.0 wt‰ (Fig. 2P), consistent with the compressive strength and anti-swelling properties.

Hereafter, GA-siTNFα-PS at a GA/PTD-sp ratio of 1/40 with optimal siRNA encapsulation, and GA-siTNFα-PS/SHE-Gel containing 3.6 wt% SH-SA, 6.0 wt% DA-OIn, and 1.0 wt‰ GA-siTNFα-PS with optimal gelation time, mechanical properties, and adhesive performance were selected for subsequent studies.

2.3. Antioxidant and anti-inflammatory ability of the GA-siTNFα-PS/SHE-Gel

Effective intracellular siRNA delivery is crucial for transfection [34,35]. Cellular uptake of GA-siTNFα-PS encapsulating Cy5-labeled siTNFα (Cy5-siTNFα) was studied. CLSM images illustrated prominent red fluorescence in cells incubated 4 h with GA-Cy5-siTNFα-PS or Cy5-siTNFα-PS and essentially no fluorescence in Cy5-siTNFα group (Fig. 3A), confirming that free siRNA hardly entered cells and polymersomes can deliver siRNA into cells. Flow cytometry study showed that the endocytosis of GA-Cy5-siTNFα-PS increased with extended incubation time (Fig. S12, Supporting Information), suggesting that prolonging residence time at the inflamed colon may improve the endocytosis of GA-siTNFα-PS in macrophages. Additionally, GA-siTNFα-PS was non-cytotoxic within the concentration range of 0–1.0 mg mL^{-1} (Fig. S13, Supporting Information).

The antioxidant ability of GA-siTNFα-PS/SHE-Gel was investigated using LPS-stimulated macrophages (LPS group), which displayed the most intense fluorescence (45.8 %) of ROS (Fig. 3B and C, Supporting Information). Following hydrogel treatment, ROS decreased from SO-Gel (38.0 %), formed by SH-SA and OIn, to SHE-Gel (22.8 %) and GA-siTNFα-PS/SHE-Gel (15.4 %). As compared to the slight ROS scavenging capacity of SO-Gel, SHE-Gel exhibited better ROS clearance ability due to its abundant catechol groups. Interestingly, GA-siTNFα-PS/SHE-Gel showed an excellent ROS-scavenging effect, stemming from the synergistic antioxidant effect of dopamine and sulfhydryl groups on hydrogel surface and gallic acid in GA-siTNFα-PS (Fig. S14, Supporting Information). Additionally, GA-siTNFα-PS significantly suppressed TNFα mRNA expression. This suppression was comparable to that observed in the siTNFα-Lipo (Lipo: Lipofectamine 2000) group, which can be attributed to the enhanced cellular uptake and antioxidant abilities of GA-siTNFα-PS (Figs. S15 and 16, Supporting Information). Meanwhile, GA-siTNFα-PS/SHE-Gel demonstrated non-cytotoxicity with GA-siTNFα-PS concentration ranging from 0.2 to 2.0 wt‰ (Fig. S17, Supporting Information).

The anti-inflammatory capacity of GA-siTNFα-PS/SHE-Gel was further assessed by evaluating the cytokine expression of M1 macrophage-related TNF-α, IL-6 and M2 macrophage-related IL-10 (Fig. 3D–F). The hydrogel demonstrated the highest capacity of TNF-α and IL-6 inhibition compared to SHE-Gel and SO-Gel, attributable to the synergistic effect of the antioxidant capabilities of DA-OIn and SH-SA in the hydrogel, along with the ROS scavenging activity and TNF-α silencing capability provided by GA-siTNFα-PS (Fig. S18, Supporting Information). Concomitantly, GA-siTNFα-PS/SHE-Gel significantly upregulated M2-related IL-10, suggesting that it exerted excellent anti-inflammatory effects by suppressing M1 macrophage polarization and promoting M2 macrophage activation.

2.4. Gastrointestinal stability and colon-responsive degradation

Resistance to gastrointestinal digestion, retention in the intestine, and specific degradation and release of drugs in the colon are essential features of oral carriers for the efficient treatment of colitis. To investigate the stability of GA-siTNFα-PS/SHE-Gel in the gastrointestinal tract, we first added the hydrogel into simulated gastric fluid (SGF) for 2 h and continuously added into simulated intestinal fluid (SIF) for 4 h, and studied the stability of GA-siTNFα-PS/SHE-Gel by monitoring of the morphology and weight. Notably, GA-siTNFα-PS has been proved to be unstable in SGF (Fig. S19, Supporting Information). Scanning electron microscopy (SEM) images showed that GA-siTNFα-PS/SHE-Gel shrank in volume and in pore size after immersing in SGF for 2 h (Fig. 4A; Fig. S20, Supporting Information). This contraction is likely attributed to protonation-induced charge neutralization and osmotic dehydration [36,37]. The volume and pore size of GA-siTNFα-PS/SHE-Gel were recovered to the initial state after incubating in SIF for 4 h. Additionally, the degradation rates of the hydrogel in SGF plus SIF was only 2.2 %, (Fig. S21, Supporting Information). These results indicate that GA-siTNFα-PS/SHE-Gel has the potential to resist degradation in the gastrointestinal tract.

The microbial-responsive degradation ability and drug release of GA-siTNFα-PS/SHE-Gel were investigated in simulated colon fluid (SCF) or SCF containing microbial-specific inulinase. SEM showed that the hydrogel swelled and the pore size increased after incubation in SCF for 4 or 12 h (Fig. 4A). However, the hydrogel structure collapsed after incubation in SCF containing inulinase for 12 h, with total weight loss of 39.5 % contrasting to 16.8 % at continuous incubation in SCF (Fig. S21, Supporting Information), while it maintained its porous structure after 12 h incubation in SCF containing other colonic enzymes, such as β-galactosidase (Fig. S22, Supporting Information). The release rate of GA-siTNFα-PS in SGF and SIF was merely 3.2 %, while 28.9 % and 64.1 % of GA-siTNFα-PS was released in 12 h in SCF and SCF plus inulinase, respectively (Fig. S23, Supporting Information). The release profile of GA-siTNFα-PS directly represents that of siTNFα, because the disulfide-crosslinked PS maintains structural integrity under physiological conditions but undergoes rapid reductive disassembly in intracellular environments [38], triggering synchronous siTNFα release. These results suggest that GA-siTNFα-PS/SHE-Gel can remain stable in the stomach and small intestine, but degrades in the colon, and that colon-specific inulinase can accelerate the degradation rate.

2.5. Efficient delivery of GA-siTNFα-PS to the inflamed colon

The *in vivo* delivery efficiency of GA-siTNFα-PS was explored using a mild colitis model established by allowing mice to drink DSS solution (3 %, w/v) for 4 days. In vivo fluorescence images of Cy5-labeled GA-

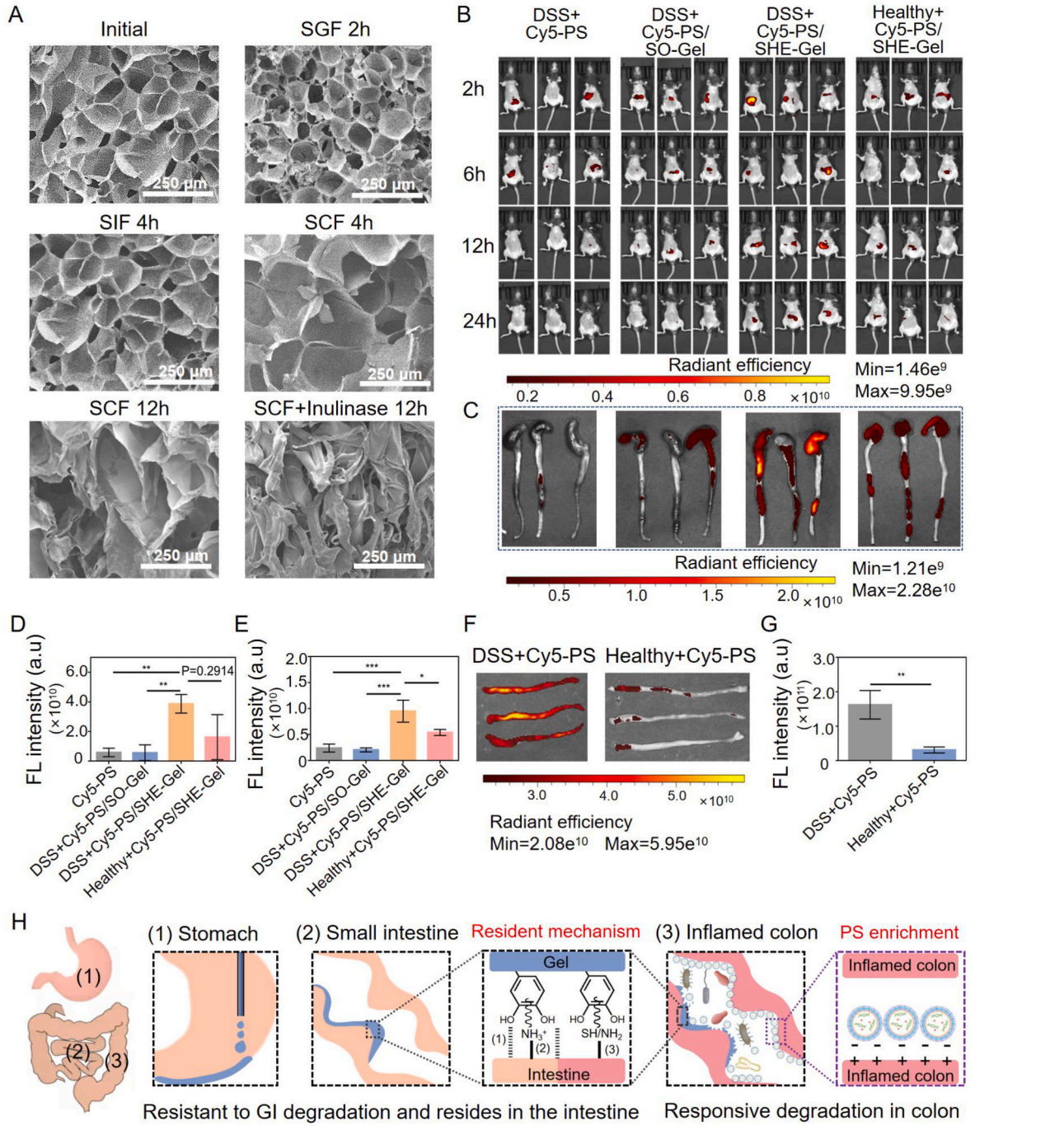

Fig. 4. GA-siTNFα-PS/SHE-Gel resists gastric juice, prolongs intestinal residence time, and ultimately degrades in a microbiome-responsive manner in the colon. A) SEM images of GA-siTNFα-PS/SHE-Gel after incubation in simulated fluid for different times. B) In vivo imaging of UC mice or healthy mice at different time points and C) ex vivo images of UC or healthy mouse colons after gavage of Cy5-labeled GA-siTNFα-PS (Cy5-PS), Cy5-PS/SO-Gel, or Cy5-PS/SHE-Gel for 24 h, as well as their corresponding fluorescence semi-quantification of (D) *in vivo* imaging of mice and (E) ex vivo images of colons (n = 3). F) In vitro images and G) fluorescence semi-quantitative analysis of UC or healthy mouse colons after culturing with Cy5-PS for 1 h and PBS wash (3 ×) (n = 3). H) The mechanism of GA-siTNFα-PS/SHE-Gel self-solidification in the stomach, retention in the intestine, and microbial-responsive degradation in colon, in which the released GA-siTNFα-PS can enrich in the inflamed colon via electrostatic interactions. (Data are presented as the mean ± SD; *, ** and *** indicate significance at $p < 0.05$, $p < 0.01$, and $p < 0.001$ respectively).

siTNFα-PS (Cy5-PS) were acquired at 2, 6, 12, and 24 h after oral administration of Cy5-PS, Cy5-PS/SO-Gel, or Cy5-PS/SHE-Gel. DSS + Cy5-PS group had a short fluorescence duration in the abdomens due to the gastrointestinal instability of Cy5-PS. The fluorescence intensities in the abdomens of mice in the DSS + Cy5-PS/SHE-Gel group maintained high levels for 24 h, compared to DSS + Cy5-PS/SO-Gel group (Fig. 4B–D), indicating that the GA-siTNFα-PS/SHE-Gel is gastrointestinal stable and has prolonged intestinal residence time, due to the catechol structure in the DA-OIn network. Moreover, the fluorescence intensity in the DSS + Cy5-PS/SHE-Gel group was higher than that in the Healthy + Cy5-PS/SHE-Gel group after 24 h of oral administration, possibly due to the specific degradation of Cy5-PS/SHE-Gel in the colon and the release of Cy5-PS homing to the inflamed colon through electrostatic absorption, while not in the healthy colon.

Fluorescence images, semi-quantification, and frozen section of colon extracts from mice after 24 h showed that the mean fluorescence intensity of colons in the DSS + Cy5-PS/SHE-Gel group was significantly higher than those of other groups (Fig. 4C–E; Fig. S24, Supporting Information). To further confirm the targeted ability of Cy5-PS to inflamed colon, the colons of UC or healthy mice were excised and incubated with Cy5-PS for 1 h Cy5-PS showed stronger fluorescence intensity in UC mice colons than in healthy mice colons (Fig. 4F and G), which was consistent with the previous reports that inflamed colon region accumulates abundant positively charged proteins and negatively charged nanoparticles can home to this region via electrostatic interactions [39–41]. These results demonstrate that GA-siTNFα-PS/SHE-Gel undergoes gastric contraction, gradual intestinal swelling, and inulinase-responsive release of GA-siTNFα-PS in the colon, ultimately enabling electrostatic targeting of the GA-siTNFα-PS to inflamed colonic sites.

Collectively, the pH and colonic microbiome responsive SHE-Gel can effectively resist the extreme acidity of the gastric juice, prolong intestinal residence time through mussel-inspired adhesion, and ultimately degrade in a microbiome-responsive manner in the colon. The released GA-siTNFα-PS can target to the inflamed colon, which contains a large number of positively charged proteins such as antimicrobial peptides

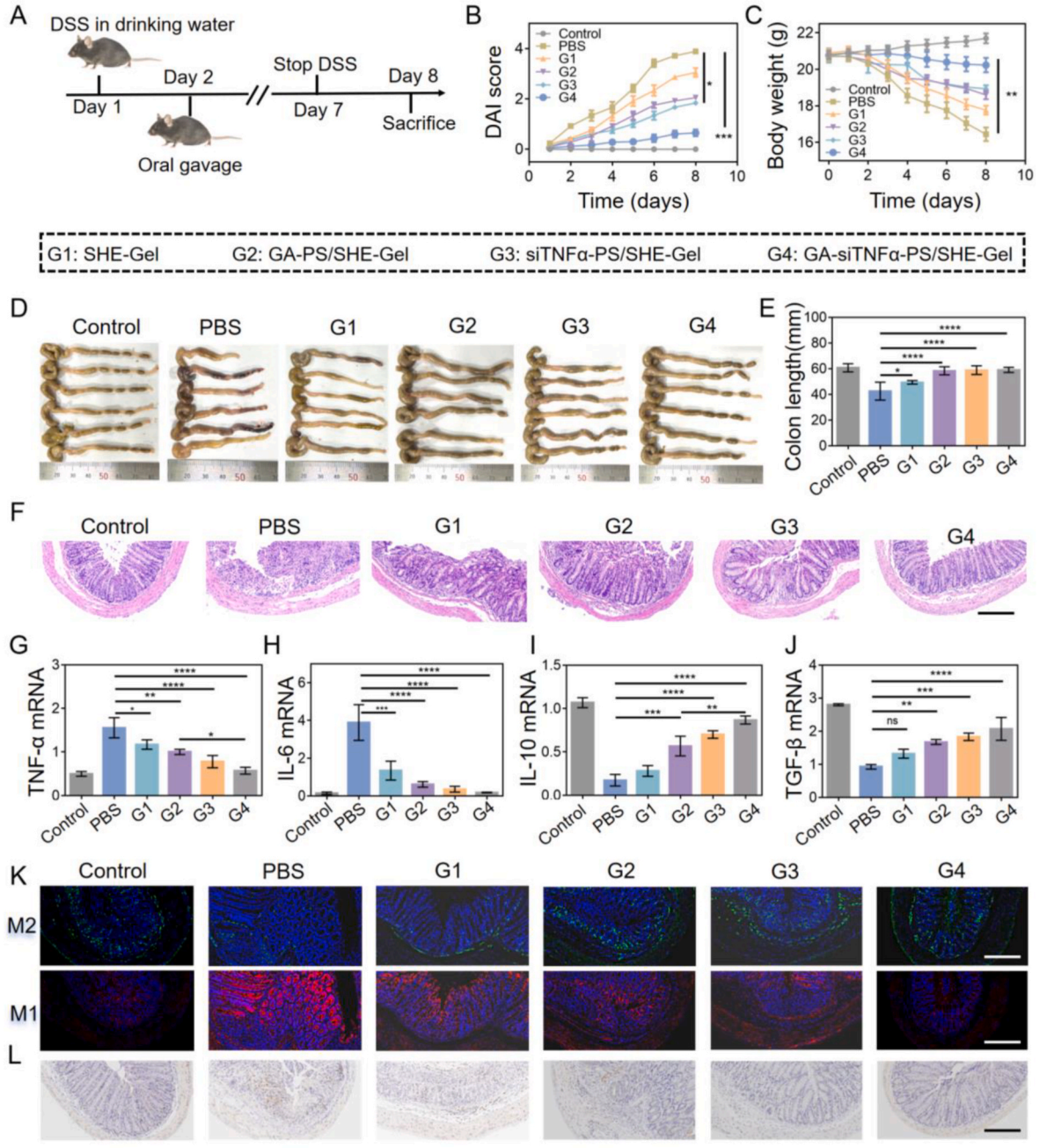

Fig. 5. Therapeutic performance of GA-siTNFα-PS/SHE-Gel in a DSS-induced UC mice model. A) Experimental design. Mice were provided 3 % DSS sterile water for 7 days. Oral administration started from the second day and mice were sacrificed on the eighth day. B) C) DAI scores and body weights (n = 6). D) E) Colon length determination (n = 6). F) Representative H&E staining images of colon tissue. H-K) Colonic mRNA levels of TNFα, IL-6, IL-10, and TGF-β(n = 3). L) Immunofluorescence analysis of M1 macrophages (CD80 (red), and 4′,6-diamidino-2-phenylindole (DAPI; blue)) and M2 macrophage (CD163 (green), and DAPI (blue)) in colon tissues. M) Immunohistochemical staining of MPO in colon tissues. Scale bars, 200 μm. (Data are presented as the mean ± SD; *, **, ***, and **** indicate significance at $p < 0.05$, $p < 0.01$, $p < 0.001$, and $p < 0.0001$, respectively).

and transferrin [41], through electrostatic interaction (Fig. 4H).

2.6. Excellent therapeutic effect of GA-siTNFα-PS/SHE-Gel in UC mice model

The DSS-induced colitis mouse model was established by allowing mice to drink DSS solution (3 %, w/v) for 7 days. Various hydrogels were orally administered on the second day (Fig. 5A). The results demonstrated that the inflammatory progression of colitis mice were suppressed after oral administration of SHE-Gel (G1), GA-PS/SHE-Gel (G2), siTNFα-PS/SHE-Gel (G3), and GA-siTNFα-PS/SHE-Gel (G4), as evidenced by lowered disease activity index (DAI) (Fig. 5B), relief of blood in stool (Fig. S25, Supporting Information), inhibition of weight loss (Fig. 5C), and recovery of colon length (Fig. 5D and E). The H&E staining results showed that GA-siTNFα-PS/SHE-Gel (G4) treatment more effectively inhibited DSS-induced colon tissue damage, demonstrated by attenuated crypt structure destruction, restored goblet cell numbers, and mitigated inflammatory cell infiltration, compared with the siTNFα-PS/SHE-Gel (G3), GA-PS/SHE-Gel (G2), and SHE-Gel groups (G1) (Fig. 5F). Additionally, G4 exhibited the strongest expression of the intestinal epithelial cell tight junction protein Zonula occludes-1 (ZO-1), similar to that of normal mice (control group) (Fig. S26, Supporting Information). The potent inflammation-suppressing effect of GA-siTNFα-PS/SHE-Gel may be attributed to the fact that GA in GA-siTNFα-PS removes intracellular ROS, which improves TNFα silencing efficiency by protecting siTNFα integrity, in addition to the antioxidant capacity of the SHE-Gel. This suggests that GA-siTNFα-PS/SHE-Gel can effectively block the DSS-induced colon inflammation process and maintain intestinal barrier function.

Next, we investigated the *in vivo* anti-inflammatory mechanism of

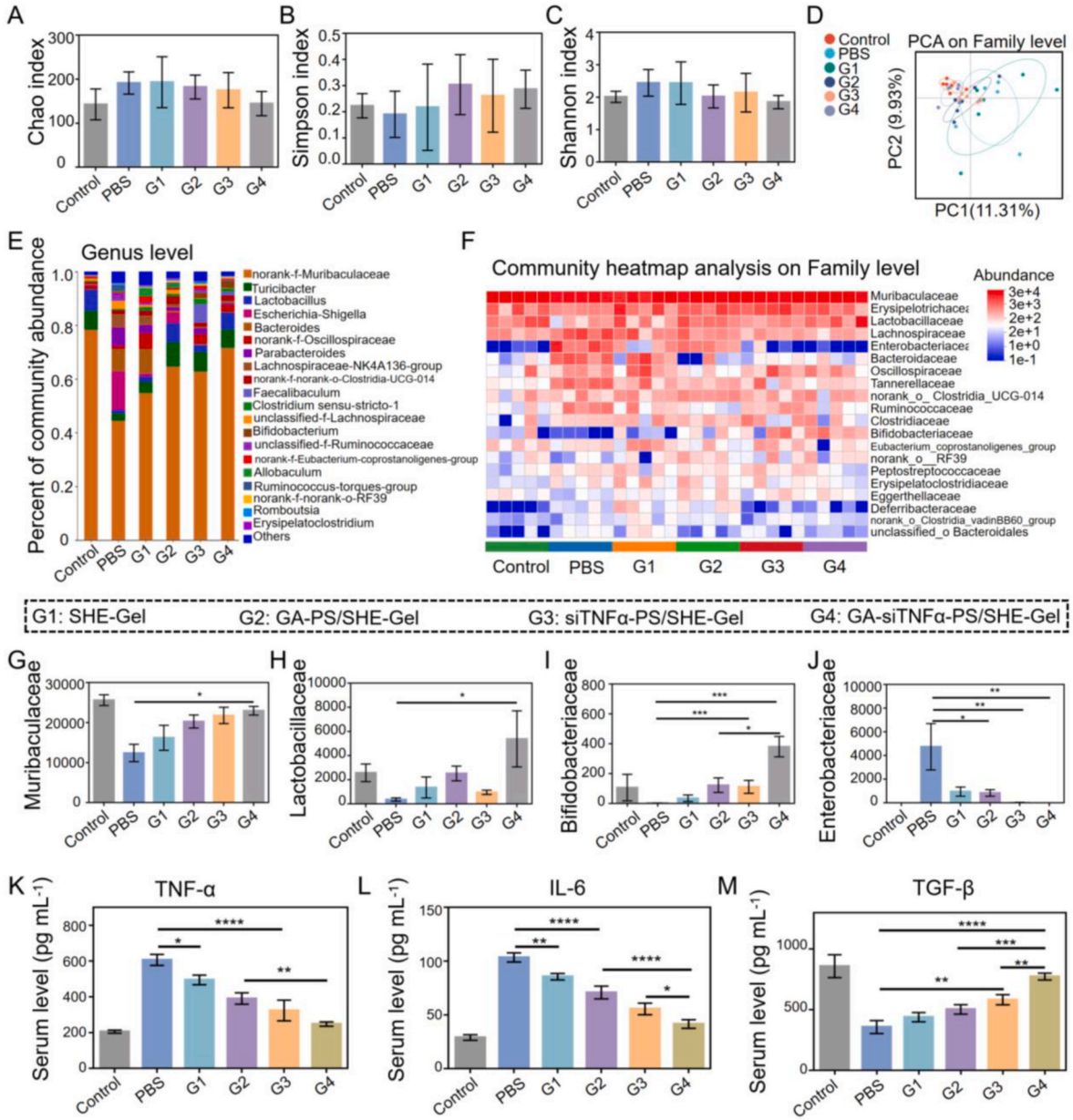

Fig. 6. Analysis of gut microbiota regulated by GA-siTNFα-PS/SHE-Gel. A) Chao, B) simpson, and C) shannon index of observed operational taxonomic units showing α-diversity of themicrobial community (n = 6). D) Principal coordinates analysis showing β-diversity of the gut microbiome (n = 6). E) Community histogram at the genus level (n = 5). F) Community heatmap analysis on family level (n = 5). Relative abundance of G) *Muribaculaceae*, H) *Lactobacillaceae*, I) *Bifidobacteriaceae*, and J) *Enterobacteriaceae* collected from F (n = 5). K–M) Serum concentrations of TNFα, IL-6, and TGF-β (n = 3). (Data are presented as the mean ± SD; *, **, ***, and **** indicate significance at $p < 0.05$, $p < 0.01$, $p < 0.001$, and $p < 0.0001$, respectively).

GA-siTNFα-PS/SHE-Gel. DSS-induced UC mice had enlarged spleens, but the increase was mitigated after GA-siTNFα-PS/SHE-Gel treatment, indicating attenuated immune activation (Fig. S27, Supporting Information). Meanwhile, colonic mRNA levels of proinflammatory cytokines (TNFα and IL-6) in GA-siTNFα-PS/SHE-Gel group were effectively suppressed (Fig. 5G and H), whereas that of anti-inflammatory factor IL-10 and the tissue repair-related cytokine transforming growth factor-β (TGF-β) increased compared with the PBS group (Fig. 5I and J). Furthermore, macrophage types in the colon were analyzed (Fig. 5K). The contents of M1 macrophages notably decreased, and the contents of M2 macrophages substantially increased after GA-siTNFα-PS/SHE-Gel treatment. Meanwhile, GA-siTNFα-PS/SHE-Gel treatment significantly attenuated the positive expression of myeloperoxidase (MPO) in DSS-induced inflammatory colon tissue (Fig 5L). These findings demonstrated that GA-siTNFα-PS/SHE-Gel effectively modulates the inflammatory response, reduces oxidative stress, and promotes the conversion of M1 to M2 macrophages to treat DSS-induced colitis.

2.7. Regulation of gut microbiota by GA-siTNFα-PS/SHE-Gel in UC mice model

Dysbiosis of the intestinal microbiota is closely associated with the development of DSS-induced colitis in mice. We next examined gut microbiome changes by 16S ribosomal RNA gene sequencing in the V3-V4 regions. There was no difference in the richness and diversity of the gut microbiome according to the chao, simpson, and shannon indexes of operational taxonomic unit (OTU) after PBS or hydrogels treatment (Fig. 6A–C). This may be due to the short duration of colitis [42]. Principal coordinate analysis (PCA) showed that GA-siTNFα-PS/-SHE-Gel (G4) significantly altered the microbial community composition of mice with DSS-induced colitis (Fig. 6D), and was similar to the control group. siTNFα-PS/SHE-Gel group (G3) and GA-PS/SHE-Gel group (G2) were close to G4, whereas SHE-Gel group (G1) showed a trend away from the DSS group and closer to G3 and G2.

The general enterobacteria composition at the genus (Fig. 6E) and family levels (Fig. 6F) are shown by bar graphs and heatmaps, respectively. The composition of the microbiome at the genus level was improved after oral administration of SHE-Gel (G1), GA-PS/SHE-Gel (G2), siTNFα-PS/SHE-Gel (G3), and GA-siTNFα-PS/SHE-Gel (G4). In particular, G4 exhibited significantly increased abundance of beneficial *norank-f-Muribaculaceae*, *Turicibacter*, and *Lactobacillus*, and a decreased relative abundance of *Escherichia-Shigella*, a harmful pathogen that causes intestinal infections and worsens enteritis. Next, several special bacteria were quantitatively analyzed at the family level (Fig. 6G–J). GA-siTNFα-PS/SHE-Gel treatment notably retained the relative abundances of *Muribaculaceae* (major intestinal microbiota that maintains the steady state of the intestine in healthy guts) [43], *Lactobacillaceae* (promotes intestinal balance and enhances immunity of the host) [44], and *Bifidobacteriaceae* (improves ulcerative colitis caused by immune system disorders) [45]. While *Enterobacteriaceae* (a common class of zoonotic pathogens or primary human pathogens) [46, 47] were markedly decreased. These results suggest that GA-siTNFα-PS/SHE-Gel positively modulates the gut microbiota by effectively promoting the growth of beneficial bacteria and reducing harmful bacteria. Additionally, the recovery of bacterial abundance was more pronounced in G2 (GA-PS/SHE-Gel) when compared with G1 (SHE-Gel), likely due to the potential flora regulation ability and anti-inflammatory effects of gallic acid [48], in addition to the flora regulation effect of inulin in SHE-Gel.

Furthermore, the effect of hydrogels on DSS-induced systemic inflammation was evaluated by measuring the levels of TNF-α, IL-6, and TGF-β in mouse serum after 7 days of treatment. The results showed that TNF-α and IL-6 increased after 7 days of DSS administration. Their levels were decreased after treatment with SHE-Gel (G1), attributed to the synergistic effect of the mild anti-inflammatory effect of SH-SA and the ROS scavenging and flora regulation of DA-OIn (Fig. 6K–M). The administration of GA-siTNFα-PS/SHE-Gel (G4) significantly inhibited the expression of TNF-α and IL-6, and improved the expression of TGF-β, showing higher efficacy than GA-PS/SHE-Gel (G2, no siRNA) and siTNFα-PS/SHE-Gel (G3, no GA). The superior systemic inflammation inhibition may be attributed to the fact that GA-siTNFα-PS/SHE-Gel not only effectively blocks the progression of inflammation but also maintains the homeostasis of gut microbiota in the ulcerative colitis model. GA-siTNFα-PS/SHE-Gel was safe *in vivo* and did not cause systemic toxicity (Fig. S28, Supporting Information).

2.8. Effective treatment of advanced colitis model by GA-siTNFα-PS/SHE-Gel combined with anti-TNFα antibody

In late-stage UC, inflammatory factor infiltration intensifies the symptom. Intravenous (iv) infliximab rapidly neutralizes circulating TNF-α, mitigating systemic inflammation faster than siRNA nanomedicines that act upstream via TNF-α mRNA silencing within inflammatory cells. Combining GA-siTNFα-PS/SHE-Gel with infliximab (iv) achieves dual-pathway blockade: the former targets localized colonic pathology, while the latter suppresses systemic inflammation. Based on this rationale, we investigated the therapeutic effects of GA-siTNFα-PS/SHE-Gel (Gel), infliximab (iv), and Gel + infliximab (iv) in an advanced colitis, established by free drinking of 3 % DSS sterile water for seven days. The treatment was started on the eighth day (Fig. 7A). Gel administration inhibited weight loss (Fig. 7B), relieved blood in stool (Fig. S29, Supporting Information), restored shortened colon length (Fig. 7C and D), and reduced spleen weight (Fig. S30, Supporting Information) in late-stage UC mice. Treatment by Gel has similar therapeutic effects to infliximab (iv), which may be attributed to the rapid ROS scavenging capability of DA in DA-OIn and GA in GA-siTNFα-PS before siTNFα transfection. Gel + infliximab treatment effectively alleviated the symptoms of late-stage UC mice, and all indicators were close to those of the normal mice (control group). H&E staining results showed that Gel + infliximab preserved colon tissue integrity and maintained goblet cell counts similar to the control group (Fig. 7E). Additionally, the expression of ZO-1 significantly increased after Gel + infliximab treatment (Fig. 7F). These findings indicate that GA-siTNFα-PS/SHE-Gel plus infliximab can effectively improve the inflammatory microenvironment and restore intestinal epithelial barrier function in an advanced colitis model.

We explored the therapeutic mechanism of Gel + infliximab. Colonic mRNA levels of M1-related proinflammatory cytokines TNFα and IL-6 in Gel + infliximab group were effectively inhibited, and the expression of M2-related IL-10 and TGF-β increased (Fig. S31, Supporting Information), which was nearing to the control group. Additionally, Gel + infliximab significantly reduced the positive expression of MPO in colon tissue compared with PBS group (Fig. 7G). These results demonstrated that Gel + infliximab can effectively treat late-stage UC mice by inhibiting oxidative stress and promoting M1 to M2 conversion.

We further analyzed the diversity of intestinal flora. Treatment by Gel + infliximab augmented the richness and diversity of the gut microbiome according to the chao, ace, and sobs indexes of OTU (Fig. 7H–K), although there was no significant difference in shannon index. PCA showed that Gel + infliximab treatment significantly changed the microbial community composition of advanced colitis mice (Fig. S32A, Supporting Information). The composition of the microbiome at the genus level in Gel + infliximab group was significantly improved and maintained a similar composition to that of the control group (Fig. S32B, Supporting Information). Next, several special bacteria were quantitatively analyzed at the family level (Fig. 7L–O; Fig. S32C, Supporting Information). Gel + infliximab treatment significantly retained the relative abundances of beneficial *Muribaculaceae*, *Akkermansiaceae*, and *Erysipelotrichaceae*. While harmful *Enterococcaceae* were markedly reduced. These results suggest that GA-siTNFα-PS/SHE-Gel combined with infliximab positively modulated the gut microbiota by increasing the abundance of beneficial bacteria and reducing harmful bacteria in an advanced colitis model. In addition, Gel + infliximab can

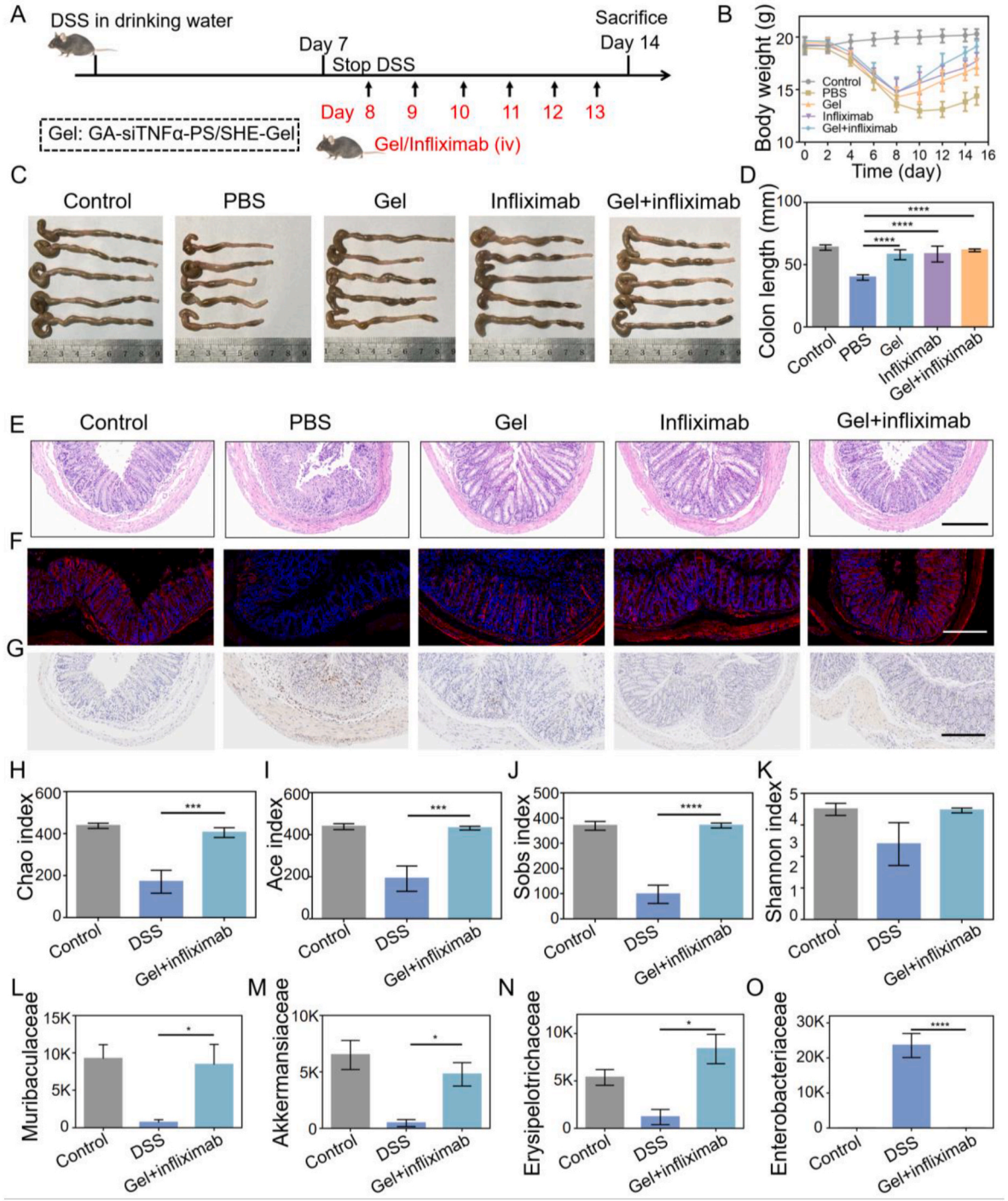

Fig. 7. Therapeutic performance of GA-siTNFα-PS/SHE-Gel plus infliximab in an advanced colitis model. A) Experimental design. Mice were provided sterile water containing 3 % DSS for 7 days. Treatment started on the 8 day and continued for 7 consecutive days. All mice were sacrificed on the 15 day. B) Daily changes in body weight were recorded (n = 5). C) D) Colon lengths were measured and analyzed (n = 5). E) Representative H&E staining images of colon tissue of each group. F) Immunofluorescence analysis of ZO-1. G) Immunohistochemical staining of MPO in colon tissue. H) Chao, I) ace, J) sobs, and K) shannon index of observed OTU (n = 5). Relative abundance of L) *Muribaculaceae*, M) *Akkermansiaceae*, N) *Erysipelotrichaceae*, and O) *Enterobacteriaceae* collected from community heatmap analysis on family level (n = 5). (Scale bars, 200 μm. Data are presented as the mean ± SD; *, ***, and **** indicate significance at $p < 0.05$, $p < 0.001$, and $p < 0.0001$, respectively).

substantially reduce the systemic proinflammatory factors TNFα and IL-6, while increase the level of TGF-β, indicating that Gel + infliximab can effectively relieve systemic inflammation (Fig. S33, Supporting Information).

In short, GA-siTNFα-PS/SHE-Gel can effectively block the progression of inflammation and maintain the homeostasis of intestinal flora in the ulcerative colitis model. The reason is that (1) the DA-OIn in SHE-Gel fermented by colonic microorganisms to produce metabolites with prebiotic activity to regulate the intestinal flora, while DA-OIn scavenging ROS in the intestine and exerting anti-inflammatory effects. (2) Lesion-enriched GA-siTNFα-PS is efficiently internalized by macrophages and release GA and siTNFα under intracellular reduction

conditions. GA has high ROS-scavenging ability, protects siTNFα during delivery, effectively silencing TNFα, and ultimately inhibits intestinal inflammation. Additionally, GA-siTNFα-PS/SHE-Gel can further combine with anti-TNFα antibody, which restores the intestinal immune and gut microbiota homeostasis in an advanced colitis mice model.

3. Conclusion

We developed oral microbiota-regulating and inflammation-targeted polymersome-hydrogels (GA-siTNFα-PS/SHE-Gel) for RNAi therapy of ulcerative colitis. GA-siTNFα-PS/SHE-Gel has several unique features: (1) it has nano-enhanced mechanical property, self-healing property, tissue adhesive property, and pH/microbial responsive property, which enable it withstand to the harsh gastrointestinal condition, adhere completely to the colon, and degrade in the colon by colon-specific inulinase; (2) DA-OIn in SHE-Gel will be fermented by colonic microorganisms to produce metabolites with prebiotic activity to regulate the intestinal flora, while scavenging ROS in the intestine and exerting anti-inflammatory effects; (3) GA-siTNFα-PS released in the colon can adhere to the inflamed sites, resulting in efficient delivery of GA-siTNFα-PS to macrophages. The released GA has high ROS-scavenging ability and protects siTNFα during delivery, effectively silencing TNFα and ultimately inhibiting the overactive intestinal immune response. GA-siTNFα-PS/SHE-Gel has antioxidant, anti-inflammatory and flora regulation property, which can not only halt the progression of DSS-induced colitis mice but also effectively restore the intestinal immune and gut microbiota homeostasis in an advanced model of colitis when combined with infliximab. In general, the polymersome-hydrogel proposed in this study provides a unique and powerful platform for designing treatments for colon diseases.

4. Experimental section

4.1. The preparation of GA-siTNFα-PS

A certain amount of GA (160 mg mL^{-1} in DMF) was added to 40 μL of PEG-P (TMC-DTC)-Spermine (PTD-sp, 40 mg mL^{-1} in DMF) solution, and stirred at room temperature for 30 min. The mixture was slowly dripped into 320 μL of PB (pH = 6.0) containing 40 μL of siTNFα (1 mg mL^{-1} in DEPC water). After stirring at room temperature for 5 min, the mixture was dialyzed (Mw cutoff: 14000 Da) in PB (pH = 6.0) for 1 h, then in a 1:1 vol mix of PB at pH 6.0 and pH 7.4 for another hour, and finally in PB (pH = 7.4) for 30 min to obtain the GA-siTNFα-PS. The preparation methods of siTNFα-PS and GA-PS are the same as that of GA-siTNFα-PS, except without GA or siTNFα. PTD-sp was synthesized according to the previous reports [49,50].

4.2. The loading efficiency of siTNFα and GA in GA-siTNFα-PS

GA-siTNFα-PS was prepared and dialyzed to remove unencapsulated siRNA and GA. The absorbance of the GA-siTNFα-PS solution was then measured at 650 nm (for Cy5-siRNA) using an Ultrafine Nucleic Acid Analyzer (Nano-400A) and at 280 nm (for GA) using a UV–Vis spectrophotometer. The encapsulation rate was calculated using pre-established standard curves of Cy5-siRNA and GA.

4.3. The preparation of hydrogels

The preparation of GA-siTNFα-PS/SHE-Gel was as follows. 50 μL GA-siTNFα-PS solution (4 mg mL^{-1}) was mixed with 30 μL DA-OIn (400 mg mL^{-1}), Then, 120 μL SH-SA (60 mg mL^{-1}) was added to the mixture and shaken immediately to form a gel. The preparation of GA-siTNFα-PS/SO-Gel was the same as that of GA-siTNFα-PS/SHE-Gel, but the DA-OIn solution was replaced with OIn solution.

4.4. Characterization

Transmission electron microscopy (TEM) images of GA-siTNFα-PS were obtained using a JEM-2100F field-emission transmission electron microscope at an acceleration voltage of 200 kV. The morphologies of the hydrogels were characterized using scanning electron microscopy (SEM, Zeiss Supra 55). Ultraviolet–visible (UV–Vis) spectroscopy was performed using a Lambda 950 UV–Vis spectrophotometer. The zeta potential of the NMs was measured using a highly sensitive zeta potential and particle size analyzer (Nano ZS). All the measurements were performed at room temperature.

4.5. Endocytosis experiments

1 mL RAW264.7 cells (1×10^5 cells mL^{-1} in DMEM) were seeded in confocal dishes and incubated for 12 h. The cell culture medium was then changed to 1 mL of fresh high-glucose DMEM medium containing Cy5-siTNFα, Cy5-siTNFα-PS, GA-Cy5-siTNFα-PS, and Cy5-siTNFα-Lipo (Cy5-siTNFα conc.: 1.33 μg $mL^{-1)}$ respectively, and incubated with the cells for 4h, 8h or 12h. The culture medium was removed, and 4,6-diamidino-2-phenylindole (DAPI; ab1041139, Abcam) was added to each well for nuclear labeling. The cells were observed using CLSM after repeated washing with phosphate-buffered saline (PBS). The cells were gently scraped and collected in 1 mL PBS solution for quantitative flow analysis.

4.6. Oxidative stress assay

RAW264.7 cells were seeded in 24-well plates with hydrogel (SO Gel, SHE Gel, and GA-siTNFα-PS/SHE-Gel) at a density of 1.5×10^4 cells per well. After cell attachment, the medium was removed and high-glucose DMEM medium containing lipopolysaccharide (LPS) (L4391, Sigma, USA) (100 ng mL^{-1}) was added and incubated with the cells for 24 h. Thereafter, the cells were washed with PBS and stained with the ROS-sensitive probe 2′,7′-dichlorodihydrofluorescein diacetate (DCFH-DA, 500 μL, 10 μM). Finally, the characteristic fluorescence of ROS in the cells was observed using a confocal laser scanning microscope (CLSM, LSM880, Zeiss, Germany) after washing the cells three times with PBS. Flow cytometry was used to quantify the intracellular ROS levels. After DCFH-DA staining, the cells were washed three times with PBS, scraped off the well, and dispersed in 1 mL PBS for detection with a flow cytometer (Cytoflex, Beckman, USA).

4.7. Anti-inflammatory activity in vitro

RAW264.7 cells were seeded in 12-well culture plates with hydrogel (SO-Gel, SHE-Gel, and GA-siTNFα-PS/SHE-Gel) at a density of 1×10^5 cells per well. After cell attachment, the medium was placed with high-glucose DMEM supplemented with LPS (100 ng mL^{-1}). After 24 h of treatment, the supernatant was collected, and inflammatory factors, including tumor necrosis factor-α (TNFα), interleukin-6 (IL-6), and interleukin-10 (IL-10), were tested by enzyme-linked immunosorbent assay (ELISA) according to the manufacturer's protocol (eBioscience).

4.8. The therapeutic effect of hydrogel in DSS-induced UC mouse model

All animal experiments were approved by the Animal Care and Use Committee of Soochow University and conducted according to the Guidelines for the Care and Use of Experimental Animals. Thirty-six mice in total were housed in a pathogen-free (SPF) environment and the animal experiments were randomized into six groups. Acute colitis was induced by administering 3 % (w/v) DSS in their drinking water for 7 days. The control group received sterile water without DSS. The remaining five groups treated with PBS (PBS group), SHE-Gel (G1), GA-PS/SHE-Gel (G2), siTNFα-PS/SHE-Gel (G3), and GA-siTNFα-PS/SHE-Gel (G4) received freshly prepared DSS solution (3 % w/v). Hydrogel gavage

treatment (200 μL) was administered on the second day of colitis induction. During this period, the mice were observed daily for fecal consistency, blood in the stool, and body weight. The disease activity index (DAI) was calculated by combining the percentage of weight loss (weight unchanged = 0, 1–5 % = 1, 5–10 % = 2, 10–15 % = 3, and greater than 15 % = 4), stool consistency (normal = 0, loose stool = 2, diarrhea = 4), and stool bleeding (normal = 0, occult blood positive = 2, overt bleeding = 4). The total score for these three criteria was divided by 3 to obtain the DAI value: DAI = (body weight index + stool shape + bleeding)/3. The mice were euthanized on the 8th day, and blood, feces, colon, and spleen were collected for further analysis.

4.9. The therapeutic effect of hydrogel in an advanced model of colitis in mice

The mice were randomly divided into five groups. The control group received sterile water without DSS, while the remaining mice were induced to acute colitis by freely drinking DSS solution for seven days. On the eighth day, the UC mice were randomly divided into four groups and administered PBS, GA-siTNFα-PS/SHE-Gel, infliximab (10 mg kg^{-1}, iv), and GA-siTNFα-PS/SHE-Gel plus infliximab (10 mg kg^{-1}, iv) by gavage for 7 consecutive days. The mice were observed daily for fecal consistency, blood in the stool, and body weight. On the 15th day, the mice were euthanized, and blood, feces, colon, and spleen were collected for further analysis.

4.10. Statistical methods

The experiments were performed at least in triplicate. The data of the experiments were presented as mean ± Standard Deviation (SD). Statistical significance among different groups with continuous variables was analyzed by the One-way analysis of variance (ANOVA) test with a value of *$p < 0.05$, **$p < 0.01$, ***$p < 0.005$ and ****$p < 0.001$.

CRediT authorship contribution statement

Huan He: Writing – original draft, Investigation, Funding acquisition, Data curation. **Xinyi Dong:** Data curation. **Li Cao:** Project administration. **Yongjie Sha:** Supervision, Methodology. **Yinping Sun:** Methodology. **Songsong Zhao:** Methodology. **Fenghua Meng:** Writing – review & editing. **Zhiyuan Zhong:** Writing – review & editing, Project administration, Funding acquisition, Conceptualization.

Ethics approval and consent to participate

All animal experiments were approved by the Animal Care and Use Committee of Soochow University (approval number: SUDA20240716A03), and all protocols of animal studies conformed to the Guide for the Care and Use of Laboratory Animals.

Declaration of competing interest

The authors declare no conflict of interest.

Acknowledgement

This work is supported by research grants from the National Natural Science Foundation of China (NSFC52033006), and the National Postdoctoral Researcher Program (GZC20241187).

Appendix A. Supplementary data

Supplementary data to this article can be found online at https://doi.org/10.1016/j.bioactmat.2025.06.039.

References

[1] T. Kobayashi, B. Siegmund, C.L. Berre, S.C. Wei, M. Ferrante, B. Shen, C. Bernstein, S. Danese, L. Peyrin-Biroulet, T. Hibi, Ulcerative colitis, Nat. Rev. Dis. Primers 6 (1) (2020) 74.
[2] T. Xiong, H. Xu, Q. Nie, B. Jia, H. Bao, H. Zhang, J. Li, Z. Cao, S. Wang, L. Wu, J. Zhang, Reactive oxygen species triggered cleavage of thioketal-containing supramolecular nanoparticles for inflammation-targeted oral therapy in ulcerative colitis, Adv. Funct. Mater. 35 (1) (2025) 2411979.
[3] Y. Ma, S. Gou, Z. Zhu, J. Sun, M. Shahbazi, T. Si, C. Xu, J. Ru, X. Shi, R. Reis, S. Kundu, B. Ke, G. Nie, B. Xiao, Transient mild photothermia improves therapeutic performance of oral nanomedicines with enhanced accumulation in the colitis mucosa, Adv. Mater. 36 (14) (2024) 2309516.
[4] S. Berger, F. Seeger, T.Y. Yu, M. Aydin, H. Yang, D. Rosenblum, L. Guenin-Macé, C. Glassman, L. Arguinchona, C. Sniezek, A. Blackstone, L. Carter, R. Ravichandran, M. Ahlrichs, M. Murphy, I. Swanson Pultz, A. Kang, A. Bera, L. Stewart, K. Christopher Garcia, S. Naik, J. Spangler, F. Beigel, M. Siebeck, R. Gropp, D. Baker, Preclinical proof of principle for orally delivered Th17 antagonist miniproteins, Cell 187 (16) (2024) 4305–4317.
[5] J. Wang, G. Kang, H. Lu, A. Marco, H. Yuan, Z. Feng, M. Gao, X. Wang, H. Wang, X. Zhang, Y. Wang, M. Zhang, P. Wang, Y. Feng, Z. Liu, X. Cao, H. Huang, Novel bispecific nanobody mitigates experimental intestinal inflammation in mice by targeting TNF-α and IL-23p19 bioactivities, Clin. Transl. Med. 14 (3) (2024) e1636.
[6] R. Mao, M. Chen, Precision medicine in IBD: genes, drugs, bugs and omics, Nat. Rev. Gastroenterol. Hepatol. 19 (2) (2022) 81–82.
[7] D. C Baumgart, C. Le Berre, Newer biologic and small-molecule therapies for inflammatory bowel disease, N. Engl. J. Med. 385 (14) (2021) 1302–1315.
[8] K. Huang, W. Hu, L.Q. Huang, Q.X. Zhou, Z.Y. Song, H.Y. Tao, B. Xu, C.Y. Zhang, Y. Wang, X.H. Xing, "Two-birds-one-stone" oral nanotherapeutic designed to target intestinal integrins and regulate redox homeostasis for UC treatment, Sci. Adv. 10 (30) (2024) eado7438.
[9] B.E. Sands, B.G. Feagan, L. Peyrin-Biroulet, S. Danese, D.T. Rubin, O. Laurent, A. Luo, D.D. Nguyen, J. Lu, M. Yen, J. Leszczyszyn, R. Kempiński, D.P. B. McGovern, C. Ma, T.E. Ritter, S. Targan, Phase 2 trial of anti-TL1A monoclonal antibody tulisokibart for ulcerative colitis, N. Engl. J. Med. 391 (12) (2024) 1119–1129.
[10] T. Chapman, C. Frias Gomes, E. Louis, J. Colombel, J. Satsangi, De-escalation of immunomodulator and biological therapy in inflammatory bowel disease, Lancet Gastroenterol. Hepatol. 5 (1) (2020) 63–79.
[11] Q. Fan, Z. Yang, Y. Li, Y. Cheng, Y. Li, Polycatechol mediated small interfering RNA delivery for the treatment of ulcerative colitis, Adv. Funct. Mater. 31 (24) (2021) 2101646–2101657.
[12] X. Zhou, M. Yu, L. Ma, J. Fu, J. Guo, J. Lei, Z. Fu, Y. Fu, Q. Zhang, C. Zhang, X. Chen, In vivo self-assembled siRNA as a modality for combination therapy of ulcerative colitis, Nat. Commun. 13 (1) (2022) 5700.
[13] H. He, Q. Qin, F. Xu, Y. Chen, S. Rao, C. Wang, X. Jiang, X. Lu, C. Xie, Oral polyphenol-armored nanomedicine for targeted modulation of gut microbiota–brain interactions in colitis, Sci. Adv. 9 (21) (2023) eadf3887.
[14] G. Han, H. Kim, H. Jang, E.S. Kim, S.H. Kim, Y. Yang, Oral TNF-α siRNA delivery via milk-derived exosomes for effective treatment of inflammatory bowel disease, Bioact. Mater. 22 (2023) 138–149.
[15] P. Guo, W. Wang, Q. Xiang, C. Pan, Y. Qiu, T. Li, D. Wang, J. Ouyang, R. Jia, M. Shi, Y. Wang, J. Li, J. Zou, Y. Zhong, J. Zhao, D. Zheng, Y. Cui, G. Ma, W. Wei, Engineered probiotic ameliorates ulcerative colitis by restoring gut microbiota and redox homeostasis, Cell Host Microbe 32 (9) (2024) 1502–1518.
[16] X. Zhang, Z. Yuan, J. Wu, Y. He, G. Lu, D. Zhang, Y. Zhao, R. Wu, Y. Lv, K. Cai, S. He, An orally-administered nanotherapeutics with carbon monoxide supplying for inflammatory bowel disease therapy by scavenging oxidative stress and restoring gut immune homeostasis, ACS Nano 17 (21) (2023) 21116–21133.
[17] C. Zhao, J. Yang, M. Chen, W. Chen, X. Yang, H. Ye, L. Wang, Y. Wang, J. Shi, F. Yue, X. Ma, Synthetic lignin-derived therapeutic nano reagent as intestinal pH-sensitive drug carriers capable of bypassing the gastric acid environment for colitis treatment, ACS Nano 17 (1) (2023) 811–824.
[18] Y. Fu, X. Zhao, L. Wang, K. Li, N. Jiang, S.T. Zhang, R.K. Wang, Y.F. Zhao, W. Yang, A gas therapy strategy for intestinal flora regulation and colitis treatment by nanogel-based multistage NO delivery microcapsules, Adv. Mater. 36 (19) (2024) 2309972.
[19] X. Ge, H. Wen, Y. Fei, R. Xue, Z. Cheng, Y. Li, K. Cai, L. Li, M. Li, Z. Luo, Structurally dynamic self-healable hydrogel cooperatively inhibits intestinal inflammation and promotes mucosal repair for enhanced ulcerative colitis treatment, Biomaterials 299 (2023) 122184.
[20] G. Zhang, D. Song, R. Ma, M. Li, B. Liu, Z. He, Q. Fu, Artificial mucus layer formed in response to ROS for the oral treatment of inflammatory bowel disease, Sci. Adv. 10 (30) (2024) eado8222.
[21] S. Liu, Y. Cao, L. Ma, J. Sun, L. Ramos-Mucci, Y. Ma, X. Yang, Z. Zhu, J. Zhang, B. Xiao, Oral antimicrobial peptide-EGCG nanomedicines for synergistic treatment of ulcerative colitis, J. Contr. Release 347 (2022) 544–560.
[22] R. Luo, J. Liu, Q. Cheng, M. Shionoya, C. Gao, R. Wang, Oral microsphere formulation of M2 macrophage-mimetic Janus nanomotor for targeted therapy of ulcerative colitis, Sci. Adv. 10 (26) (2024) eado6798.
[23] B. Li, X. Li, X. Chu, P. Lou, Y. Yuan, A. Zhuge, X. Zhu, Y. Shen, J. Pan, L. Zhang, L. Li, Z. Wu, Micro-ecology restoration of colonic inflammation by in-Situ oral delivery of antibody-laden hydrogel microcapsules, Bioact. Mater. 15 (2022) 305–315.
[24] K. Han, J. Nam, J. Xu, X. Sun, X. Huang, O. Animasahun, A. Achreja, J.H. Jeon, B. Pursley, N. Kamada, G.Y. Chen, D. Nagrath, J.J. Moon, Generation of systemic

antitumour immunity via the in situ modulation of the gut microbiome by an orally administered inulin gel, Nat. Biomed. Eng. 5 (11) (2011) 1377–1388.
[25] M.Y. Li, J.Q. Duan, X.H. Wang, M. Liu, Q.Y. Yang, Y. Li, K. Cheng, H.Q. Liu, F. Wang, Inulin inhibits the inflammatory response through modulating enteric glial cell function in type 2 diabetic mellitus mice by reshaping intestinal flora, ACS Omega 8 (40) (2023) 36729–36743.
[26] Z. Zhang, Y. Pan, Z. Guo, X. Fan, Q. Pan, W. Gao, K. Luo, Y. Pu, B. He, An olsalazine nanoneedle-embedded inulin hydrogel reshapes intestinal homeostasis in inflammatory bowel disease, Bioact. Mater. 33 (2024) 71–84.
[27] G.W. Liu, M.J. Pickett, J.L.P. Kuosmanen, K. Ishida, W.A.M. Madani, G.N. White, J. Jenkins, S. Park, V.R. Feig, M. Jimenez, C. Karavasili, N.B. Lal, M. Murphy, A. Lopes, J. Morimoto, N. Fitzgerald, J.H. Cheah, C.K. Soule, N. Fabian, A. Hayward, R. Langer, G. Traverso, Drinkable in situ-forming tough hydrogels for gastrointestinal therapeutics, Nat. Mater. 23 (9) (2024) 1292–1299.
[28] L.A. Houghton, N.W. Read, R. Heddle, G.J. Maddern, J. Downton, J. Toouli, J. Dent, Relationship of the motor activity of the antrum, pylorus, and duodenum to gastric emptying of a solid-liquid mixed meal, Gastroenterology 94 (1988) 1276.
[29] C. Lian, J. Liu, W. Wei, X. Wu, T. Goto, H. Li, R. Tu, H. Dai, Mg-gallate metal-organic framework-based sprayable hydrogel for continuously regulating oxidative stress microenvironment and promoting neurovascular network reconstruction in diabetic wounds, Bioact. Mater. 38 (2024) 181–194.
[30] Y. Zhong, F. Meng, W. Zhang, B. Li, J. Hest, Z. Zhong, CD44-targeted vesicles encapsulating granzyme B as artificial killer cells for potent inhibition of human multiple myeloma in mice, J. Contr. Release 320 (2020) 421–430.
[31] Y. Jiang, N. Krishnan, J. Heo, R. Fang, L. Zhang, Nanoparticle-hydrogel superstructures for biomedical applications, J. Contr. Release 324 (2020) 505–521.
[32] Q. Guo, G. Zou, X. Qian, S. Chen, H. Gao, J. Yu, Hydrogen-bonds mediate liquid-liquid phase separation of mussel derived adhesive peptides, Nat. Commun. 13 (1) (2022) 5771.
[33] Y. Jiang, X. Zhang, W. Zhang, M. Wang, L. Yan, K. Wang, L. Han, X. Lu, Infant skin friendly adhesive hydrogel patch activated at body temperature for bioelectronics securing and diabetic wound healing, ACS Nano 16 (6) (2022) 8662–8676.
[34] Z. Pan, K. Xu, G. Huang, H. Hu, H. Yang, H. Shen, K. Qiu, C. Wang, T. Xu, X. Yu, J. Fang, J. Wang, Y. Lin, J. Dai, Y. Zhong, H. Song, S. Zhu, S. Wang, Z. Zhou, C. Sun, Z. Tang, S. Liao, G. Yang, Z. You, X. Dai, Z. Mao, Pyroptotic-spatiotemporally selective delivery of siRNA against pyroptosis and autoimmune diseases, Adv. Mater. 36 (38) (2024) 2407115.
[35] Y. Wei, X. Li, J. Lin, Y. Zhou, J. Yang, M. Hou, F. Wu, J. Yan, C. Ge, D. Hu, L. Yin, Oral delivery of siRNA using fluorinated, small-sized nanocapsules toward anti-inflammation treatment, Adv. Mater. 35 (11) (2023) 2206821.
[36] S. Eichler, O. Ramon, Y. Cohen, S. Mizrahi, Swelling and contraction driven mass transfer processes during osmotic dehydration of uncharged hydrogels, Int. J. Food Sci. Technol. 37 (3) (2002) 245–253.
[37] M. George, T.E. Abraham, pH sensitive alginate–guar gum hydrogel for the controlled delivery of protein drugs, Int. J. Pharm. 335 (2007) 123–129.
[38] Y. Zou, J. Wei, Y. Xia, F. Meng, J. Yuan, Z. Zhong, Targeted chemotherapy for subcutaneous and orthotopic non-small cell lung tumors with cyclic RGD-functionalized and disulfide-crosslinked polymersomal doxorubicin, Signal Transduct. Targeted Ther. 32 (2018), https://doi.org/10.1038/s41392-018-0032-7.
[39] S. Zhao, Y. Li, Q. Liu, S. Li, Y. Cheng, C. Cheng, Z. Sun, Y. Du, C. Butch, H. Wei, An orally administered CeO_2@montmorillonite nanozyme targets inflammation for inflammatory bowel disease therapy, Adv. Funct. Mater. 30 (45) (2020) 2004692.
[40] Y. Feng, X. Luo, Z. Li, X. Fan, Y. Wang, R. He, M. Liu, A ferroptosis-targeting ceria anchored halloysite as orally drug delivery system for radiation colitis therapy, Nat. Commun. 14 (2023) 5083.
[41] S. Zhang, R. Langer, G. Traverso, Nanoparticulate drug delivery systems targeting inflammation for treatment of inflammatory bowel disease, Nano Today 16 (2017) 82–96.
[42] H. Liu, Z. Cai, F. Wang, L. Hong, L. Deng, J. Zhong, Z. Wang, W. Cui, Colon-targeted adhesive hydrogel microsphere for regulation of gut immunity and flora, Adv. Sci. 8 (18) (2021) 2101619.
[43] Y. Zhu, B. Chen, X. Zhang, M.T. Akbar, T. Wu, Y. Zhang, L. Zhi, Q. Shen, Exploration of the muribaculaceae family in the gut microbiota: diversity, metabolism, and function, Nutrients 16 (16) (2024) 2660.
[44] R. Dias, C.B. Pereira, R. Pérez-Gregorio, N. Mateus, V. Freitas, Recent advances on dietary polyphenol's potential roles in celiac disease, Trends Food Sci. Technol. 107 (2021) 213–225.
[45] S. Singh, R. Bhatia, P. Khare, S. Sharma, S. Rajarammohan, M. Bishnoi, S. K. Bhadada, S.S. Sharma, J. Kaur, K.K. Kondepudi, Anti-inflammatory bifidobacterium strains prevent dextran sodium sulfate induced colitis and associated gut microbial dysbiosis in mice, Sci. Rep. 10 (1) (2020) 18597.
[46] M.I. Moreira de Gouveia, A. Bernalier-Donadille, G. Jubelin, Enterobacteriaceae in the human gut: dynamics and ecological roles in health and disease, Biology 13 (3) (2024) 142.
[47] H.M. Wexler, Bacteroides: the good, the bad, and the nitty-gritty, Clin. Microbiol. Rev. 20 (4) (2007) 593–621.
[48] Z. Wu, S. Huang, T. Li, N. Li, D. Han, B. Zhang, Z.Z. Xu, S. Zhang, J. Pang, S. Wang, G. Zhang, J. Zhao, J. Wang, Gut microbiota from green tea polyphenol-dosed mice improves intestinal epithelial homeostasis and ameliorates experimental colitis, Microbiome 9 (1) (2021) 184.
[49] Y. Zou, F. Meng, C. Deng, Z. Zhong, Robust, tumor-homing and redox-sensitive polymersomal doxorubicin: a superior alternative to doxil and caelyx, J. Contr. Release 239 (2016) 149–158.
[50] G. Cui, Y. Sun, L. Qu, C. Shen, Y. Sun, F. Meng, Y. Zheng, Z. Zhong, Uplifting antitumor immunotherapy with lymph-node-targeted and ratio-controlled codelivery of tumor cell lysate and adjuvant, Adv. Healthcare Mater. 13 (17) (2024) 2303690.